How to cite: Angew. Chem. Int. Ed. 2024, e202411861
doi.org/10.1002/anie.202411861

Starphene Chemistry Hot Paper

[19]Starphene: Combined In-Solution and On-Surface Synthesis Towards the Largest Starphene

Javier Besteiro-Sáez, Luis M. Mateo, Sergio Salaverría, Tao Wang, Paula Angulo-Portugal, Jan Patrick Calupitan, Jonathan Rodríguez-Fernández, Amador García-Fuente, Jaime Ferrer, Dolores Pérez, Martina Corso, Dimas G. de Oteyza,* and Diego Peña**

Abstract: Starphenes are structurally appealing three-fold symmetric polycyclic aromatic compounds with potential interesting applications in molecular electronics and nanotechnology. This family of star-shaped polyarenes can be regarded as three acenes that are connected through a single benzene ring. In fact, just like acenes, unsubstituted large starphenes are poorly soluble and highly reactive molecules under ambient conditions making their synthesis difficult to achieve. Herein, we report two different synthetic strategies to obtain a starphene formed by 19 *cata*-fused benzene rings distributed within three hexacene branches. This molecule, which is the largest starphene that has been obtained to date, was prepared by combining solution-phase and on-surface synthesis. [19]Starphene was characterized by high-resolution scanning tunneling microscopy (STM) and spectroscopy (STS) showing a remarkable small HOMO-LUMO transport gap (0.9 eV).

Introduction

In 1968, Clar coined the term starphene to refer to benzologues of triphenylene, in which three acene branches are annellated to a central ring and radiate outwards linearly.[1] For example, [10]starphene refers to a molecule formed by three anthracenes that are linearly fused to a central six-membered ring. The three-fold structure of starphenes gives rise to appealing optoelectronic properties that render these compounds attractive for their application in organic electronics,[2] and, more recently, as unimolecular logic gates.[3]

Just like acenes,[4] starphenes possess small HOMO (Highest Occupied Molecular Orbital)-LUMO (Lowest Unoccupied Molecular Orbital) gaps and a limited number of Clar sextets regardless of their size (one per acene arm), endowing them a higher reactivity as their size increases. Besides the high reactivity under ambient conditions of both large acenes and starphenes, another challenge related with the synthesis of these molecules is the lack of solubility that arises from a strong intermolecular π-π stacking.

For structurally complex and/or large starphenes, two predominant synthetic strategies have been established: (1) Pd-catalyzed [2+2+2] cycloaddition reaction of in situ generated arynes,[5] and (2) Ni-mediated Yamamoto coupling of *ortho*-dibromoarene derivatives.[6] By using such strategies and introducing solubilizing groups at the molecular skeleton of the starphenes, the lack of solubility could be overcome in many cases. For example, *n*-butyl[7] or hexyloxy[8] groups were introduced at the peripheral positions of [7]starphene, leading to improved solubility and

[*] J. Besteiro-Sáez, Dr. L. M. Mateo, Prof. Dr. D. Pérez, Prof. Dr. D. Peña
Centro de Investigación en Química Biolóxica e Materiais Moleculares (CiQUS) and Departamento de Química Orgánica, Universidade de Santiago de Compostela, 15782 Santiago de Compostela, Spain
E-mail: diego.pena@usc.es

S. Salaverría, Dr. D. G. de Oteyza
Nanomaterials and Nanotechnology Research Center (CINN), CSIC-UNIOVI-PA, 33940 El Entrego, Spain
E-mail: d.g.oteyza@cinn.es

Dr. T. Wang, Dr. M. Corso, Dr. D. G. de Oteyza
Donostia International Physics Center, 20018 San Sebastián, Spain

P. Angulo-Portugal, Dr. J. P. Calupitan, Dr. M. Corso
Centro de Física de Materiales (CFM-MPC), CSIC-UPV/EHU, Donostia, 20018 San Sebastián, Spain

Dr. J. P. Calupitan
Institut Parisien de Chimie Moléculaire (IPCM)
Sorbonne Université, CNRS
F-75005 Paris, France

Dr. J. Rodríguez-Fernández, Dr. A. García-Fuente, Prof. Dr. J. Ferrer
Physics Department, University of Oviedo, 33007 Oviedo, Spain
E-mail: garciaamador@uniovi.es

Prof. Dr. D. Peña
Oportunius, Galician Innovation Agency (GAIN)
15702 Santiago de Compostela, Spain

© 2024 The Author(s). Angewandte Chemie International Edition published by Wiley-VCH GmbH. This is an open access article under the terms of the Creative Commons Attribution Non-Commercial NoDerivs License, which permits use and distribution in any medium, provided the original work is properly cited, the use is non-commercial and no modifications or adaptations are made.

© 2024 The Author(s). Angewandte Chemie International Edition published by Wiley-VCH GmbH

stability. Likewise, bulky triisopropylsilyl groups were used by Bunz and co-workers to stabilize and solubilize [13]- and [16]starphene.[9] Unfortunately, larger starphenes with more extended π-conjugation and stronger π-π stacking interactions require even bulkier solubilizing groups, which might complicate their synthesis. In addition, these bulky substituents can affect the supra-molecular packing and the interaction with surfaces, which would influence crucial electronic properties when it comes to device fabrication and single-molecular electronics.

Over the past decades, on-surface synthesis (OSS) in ultra-high vacuum (UHV) conditions has emerged as a powerful alternative for the preparation of such structures that are elusive for the more classical solution-based approach.[10] In this strategy, the desired structures are directly formed on atomically clean metal surfaces, starting from appropriately designed molecular precursors. Thanks to the stabilizing effect of the surface and the ultra-high vacuum environment, highly reactive and/or insoluble compounds can be prepared and studied.[11] Moreover, OSS allows the use of local probe techniques, such as scanning tunneling microscopy (STM), atomic force microscopy (AFM) and scanning tunneling spectroscopy (STS), which provide an in-depth structural and electronic characterization of the formed structures – down to sub-atomic resolution.[12] Using OSS, Fasel and co-workers reported the synthesis of [13]starphene from *ortho*-dibromotetracene,[13] while a few years later [16]starphene was reported by Gourdon, Jancarik and co-workers, which is the largest unsubstituted starphene reported to date.[14]

Herein, we present the combined in-solution and on-surface synthesis and characterization of [19]starphene **1**, obtained from an appropriately designed hexaepoxystarphene **2** (Scheme 1). The synthesis of **2** was carried out both in-solution (from the corresponding *o*-trimethylsilylaryl triflate **3**) and on-surface (from the corresponding *o*-dibromo derivative **4**). By means of on-surface deoxygenation, we were then able to prepare the fully planar unsubstituted [19]starphene **1** on Au(111), which was characterized by means of high-resolution STM and STS. Notably, the spectroscopic data show a HOMO-LUMO transport gap (0.9 eV) that is significantly reduced with regard to that of each of its branches (hexacene, 1.8 eV)[15] and of [16]starphene (1.5 eV).[14] To the best of our knowledge, [19]starphene **1** is the largest unsubstituted starphene that has been obtained to date, and its HOMO-LUMO gap is below that of any reported acene.[16]

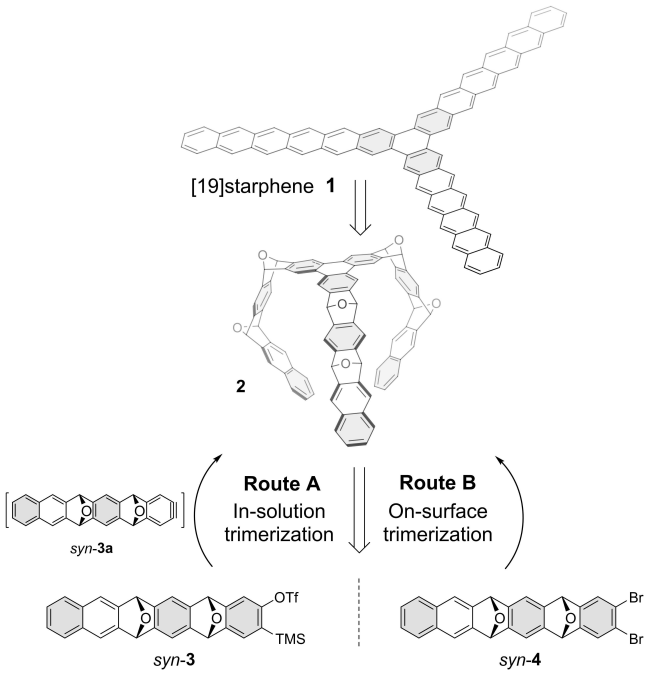

Scheme 1. Retrosynthetic route for the combined in-solution and on-surface synthesis of [19]starphene **1**.

Results and Discussion

In-Solution Synthesis of Hexaepoxystarphene 2

Our first approach towards [19]starphene was inspired by the work of Gourdon, Jancarik and co-workers, who recently reported the synthesis and characterization of [16]starphene.[14] In that work, [16]starphene was prepared in the solid state from a tri-carbonylated molecular precursor and subsequently transferred onto Au(111) by means of atomic layer injection (ALI). In the herein reported approach, which takes advantage of our experience in the preparation of large acenes,[17] we decided to design and prepare a suitable epoxide-bearing precursor **2** for its on-surface deoxygenation to give **1** (Scheme 1).

Compound **2**, precursor of [19]starphene, was first prepared by Pd-catalyzed cyclotrimerization of aryne *syn*-**3a**, which was generated from triflate **3** by fluoride-induced elimination. The aryne precursor **3** was obtained by two sequential Diels-Alder reactions between isobenzofurans and in situ generated arynes (Route A, Scheme 2). Starting from *o*-trimethylsilylnaphthyl triflate **5**, fluoride-induced generation of naphthyne **5a** and trapping with isobenzofuran **6**[18] led to the isolation of compound **7** in 90 % yield. Then, *n*-BuLi-induced generation of aryne **7a** and trapping with isobenzofuran **8** afforded triflate **3** as a mixture of two diastereoisomers in 84 % combined yield (*syn*/*anti* ratio 2:1). Both isomers (*syn*- and *anti*-**3**) were separated by means of column chromatography, and the stereochemical assignment was confirmed by single crystal X-ray diffraction (see Supporting Information). Notably, we decided to continue the synthesis with *syn*-**3** due to its presumably favorable geometry for the final on-surface reaction.[14]

Finally, fluoride-induced elimination of triflate *syn*-**3** led to the generation of aryne *syn*-**3a**, which, in the presence of catalytic amounts of a Pd complex, gave **2** in low yield (5 %) by means of [2+2+2]cycloaddition (Scheme 2).[5,19] Despite the best of our efforts, all attempts to separate both chair- and table-like diastereoisomers of compound **2** by column chromatography and/or size exclusion chromatography were unsuccessful. Also, the characterization of the mixture of isomers was hampered by significant signal broadening in ^{1}H

© 2024 The Author(s). Angewandte Chemie International Edition published by Wiley-VCH GmbH

15213773, 0, Downloaded from https://onlinelibrary.wiley.com/doi/10.1002/anie.202411861 by Uni Santiago Compostela, Wiley Online Library on [11/12/2024]. See the Terms and Conditions (https://onlinelibrary.wiley.com/terms-and-conditions) on Wiley Online Library for rules of use; OA articles are governed by the applicable Creative Commons License

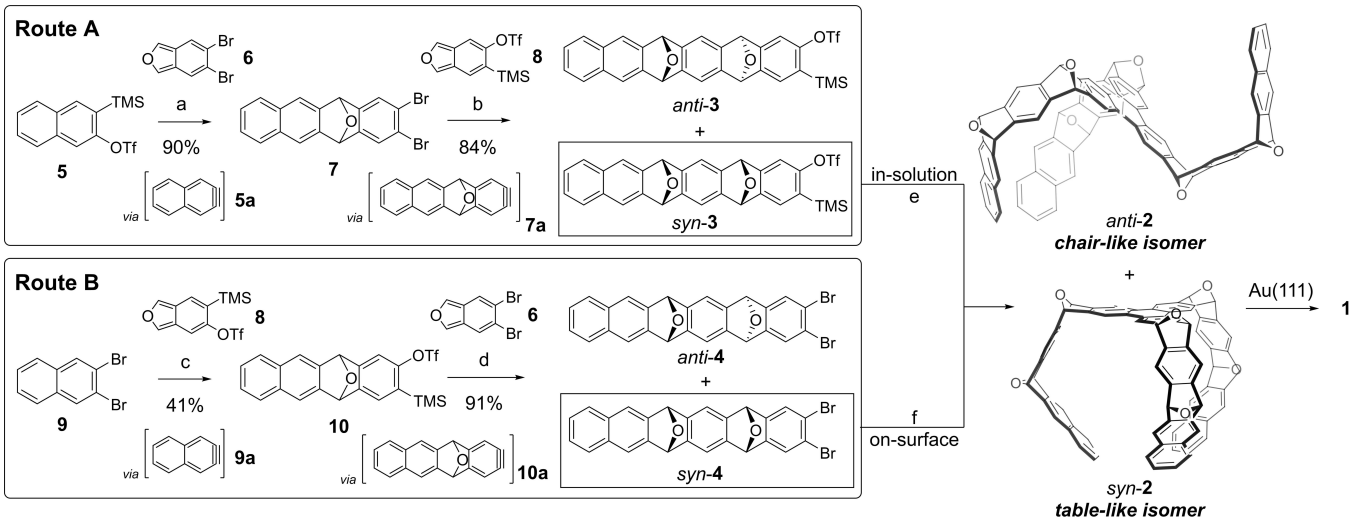

Scheme 2. a) CsF, DCM/ACN (1:1), 45 °C overnight; b) *n*-BuLi, toluene, −18 °C to r.t., overnight; c) *n*-BuLi, toluene, −18 °C to r.t., overnight; d) CsF, DCM/ACN (1:1), 45 °C overnight; e) CsF, cat. $Pd_2(dba)_3$, THF/ACN 1:1, 60 °C, overnight; f) see the main text for details.

NMR signals. However, the presence of **2** was proven by MALDI-TOF, where the molecular mass at 1074 was detected with the expected isomeric ratio (See SI, Figure S10). With this [19]strarphene precursor in hands we decided to test the on-surface deoxygenation.

On-Surface Deoxygenation of 2

The [19]starphene precursor **2** could not be deposited from a conventional Knudsen cell because it thermally decomposed before its sublimation. As an alternative approach, the precursors were deposited onto Au(111) by flash evaporation under UHV conditions. That is, small amounts of precursor powder are placed onto a Si wafer, which can be heated to high temperatures (>500 °C) very fast by turning on a current flow through the wafer. This "instant" heating under UHV has been shown to allow the sublimation of large molecules before their decomposition. A representative STM image obtained on an as-prepared sample is shown in Figure 1a. Although most molecules decomposed into fragments, a few intact precursors still

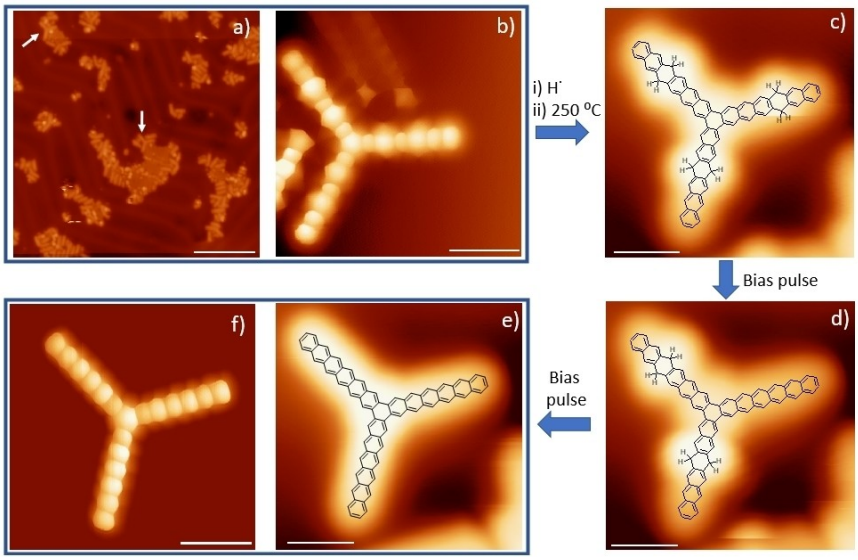

Figure 1. a) Large-scale STM image of the sample prepared by flash evaporation of the starphene precursor **2**. Most of the precursors dissociated into fragments. Only few trimer species were observed on the sample, as marked by the white arrows. b) BR-STM image of one of the intact precursors **2**, with the epoxy-functionalized rings appearing larger in size. c) STM image of one of the molecules after hydrogenation and annealing to 250 °C. d) Same molecule as panel c) after pulsing on the upper-right arm. e) Same molecule as panels c) and d) after pulsing on the remaining arms. f) BR-STM image of one of the obtained [19]starphene molecule **1**. Scale bars: a) 10 nm, b–f) 1 nm.

© 2024 The Author(s). Angewandte Chemie International Edition published by Wiley-VCH GmbH

15213773, 0, Downloaded from https://onlinelibrary.wiley.com/doi/10.1002/anie.202411861 by Uni Santiago Compostela, Wiley Online Library on [11/12/2024]. See the Terms and Conditions (https://onlinelibrary.wiley.com/terms-and-conditions) on Wiley Online Library for rules of use; OA articles are governed by the applicable Creative Commons License

survived, marked by white arrows. A zoom into one of the molecules is depicted in Figure 1b, where the six epoxy-functionalized rings of compound **2** can be clearly distinguished by bond-resolving STM (BR-STM) with CO-functionalized probes, appearing larger than the rest of the rings. Unfortunately, removal of the epoxy groups by annealing treatment or tip-induced manipulation to obtain [19]starphene **1** turned out to be extremely inefficient, with many of these groups probably turning into carbonyl groups (Figure S20). Instead, inspired in our previous works on on-surface reduction,[12c,20] we treated these samples with atomic hydrogen, followed by post-annealing treatments to 250 °C. This protocol removes the epoxy groups and only leaves few partially hydrogenated rings behind (typically one per arm, Figure 1c).

This on-surface hydrogenation causes partial planarization of the molecule, allowing better adsorption on the surface. Different from the carbonyl groups,[21] additional hydrogens can be easily removed by a bias pulse larger than 2 V (Figure 1d–e),[14,22] generating the final product, namely purely sp^2-hybridized [19]starphene **1** (Figure 1f).

On-Surface Synthesis of [19]Starphene via syn-4

Despite the successful synthesis of **1** following Route A (Scheme 2), the global yield obtained with this approach was extremely low, mostly due to the inefficient in-solution synthesis of precursor **2** as well as its uncontrollable flash evaporation to perform the on-surface experiments. In order to overcome these problems, and inspired by the successful on-surface synthesis of smaller starphenes from *ortho*-dihalogenated acenes,[13,23] we decided to attempt the preparation of [19]starphene **1** from dibromo derivative *syn*-**4**. Similarly to the synthesis of compound **3**, hexacene derivative **4** was also obtained by two sequential Diels-Alder reactions between isobenzofurans and in situ generated arynes (Route B, Scheme 2). Starting from commercially available 2,3-dibromonaphthalene (**9**), we obtained **4** in two steps as a mixture of two diastereoisomers (*syn*/*anti* ratio 2:1), which were again separated by careful column chromatography. Then, *syn*-**4** was sublimed from a Knudsen cell at around 220 °C. Deposition onto Au(111) held at room temperature followed by a post-annealing at 230 °C to trigger the Ullmann coupling reactions results again in a very low yield of trimer products (~6 %) (Figure S21a–b). Instead, the clearly dominant product stems from a dimerization reaction. In addition, many of the epoxy groups present on the precursor molecules transformed into carbonyl groups upon annealing, which were difficult to be removed by tip manipulation or further annealing treatment.[21] Thus, no [19]starphene, as a globally sp^2-hybridized product, was obtained by this synthetic protocol.

However, an improved yield of the trimer was obtained depositing the precursor directly on a preheated Au(111) substrate (Figure S21c–d). Besides, this alternative protocol also promotes the dissociation of epoxy groups from the acene backbone,[17] forming [19]starphene. Following this modified procedure, the deposition of precursor *syn*-**4** on Au(111) held at 200 °C forms symmetric trimers in ~25 % yield. Although most of these trimers still contain a few surviving carbonyl or epoxy group, [19]starphenes were also obtained readily from this growth process in a 5 % estimated yield (Figure S21d). It should be noted that this yield could be further improved using a combined hydrogenation and annealing treatment as described previously for the on-surface deoxygenation of **2**.

On-Surface Characterization of [19]Starphene

In the following we provide a detailed analysis of [19]starphene's electronic properties. STS allows us to assess the energy and the spatial distribution of the low energy molecular orbitals. Point spectra acquired at the end of the acene arms in an off-axis position provide a stronger signal of the occupied molecular states (blue curve in Figure 2b), whereas the spectra acquired on the arm's axis provide a stronger signal of the unoccupied states (red curve in Figure 2b). This is directly related with the spatial distribution of the associated orbitals, as revealed by the conductance maps (Figure 2c). Within the probed energy range, three resonances are observed for the occupied states. The first resonance at −0.36 eV is assigned to HOMO. The second resonance at −0.64 eV is assigned to the degenerate HOMO-1 and HOMO-2, and the third, broader resonance around −1.5 eV is assigned to the quasi-degenerate HOMO-3, convoluted with the degenerate HOMO-4 and HOMO-5. For the unoccupied states, we observe two distinct states and the onset of another one, respectively, assigned to LUMO (0.54 eV), to the degenerate LUMO + 1 and LUMO + 2 (1.20 eV), and to the onset of the LUMO + 3, possibly convoluted with the degenerate LUMO + 4 and LUMO + 5. In addition to the good match between the calculated molecular orbitals (Figure 2d) and the conductance maps, our measurements precisely mimic the same molecular orbitals measured on the smaller sister-molecule [16]starphene,[14] but with one more node on each orbital, as expected for the additional ring on each arm.

We now compare the measured HOMO-LUMO gap of **1** on Au(111) ($E_G = 0.9$ eV) with that of closely related molecules (Figure 2e), namely smaller starphenes[14,23] and acenes that have been synthesized and characterized to date on Au(111).[16,24] The comparison with [10]starphene and [16]starphene reveals an approximately linear decrease of the gap with additional rings. Most interestingly, the HOMO-LUMO gap of starphenes is systematically lower than the gap of the acenes that form each of its arms, which supports that the arms are partially conjugated. In particular, the gap of [19]starphene is lower than that of any reported acene, regardless of its size (Figure 2e).

Theory Insight and Extrapolation to Larger Starphenes

In order to expand the comparison to a larger range of sizes and to obtain a better understanding of these molecular systems, we have performed theoretical calculations (see

© 2024 The Author(s). Angewandte Chemie International Edition published by Wiley-VCH GmbH

15213773, 0, Downloaded from https://onlinelibrary.wiley.com/doi/10.1002/anie.202411861 by Uni Santiago Compostela, Wiley Online Library on [11/12/2024]. See the Terms and Conditions (https://onlinelibrary.wiley.com/terms-and-conditions) on Wiley Online Library for rules of use; OA articles are governed by the applicable Creative Commons License

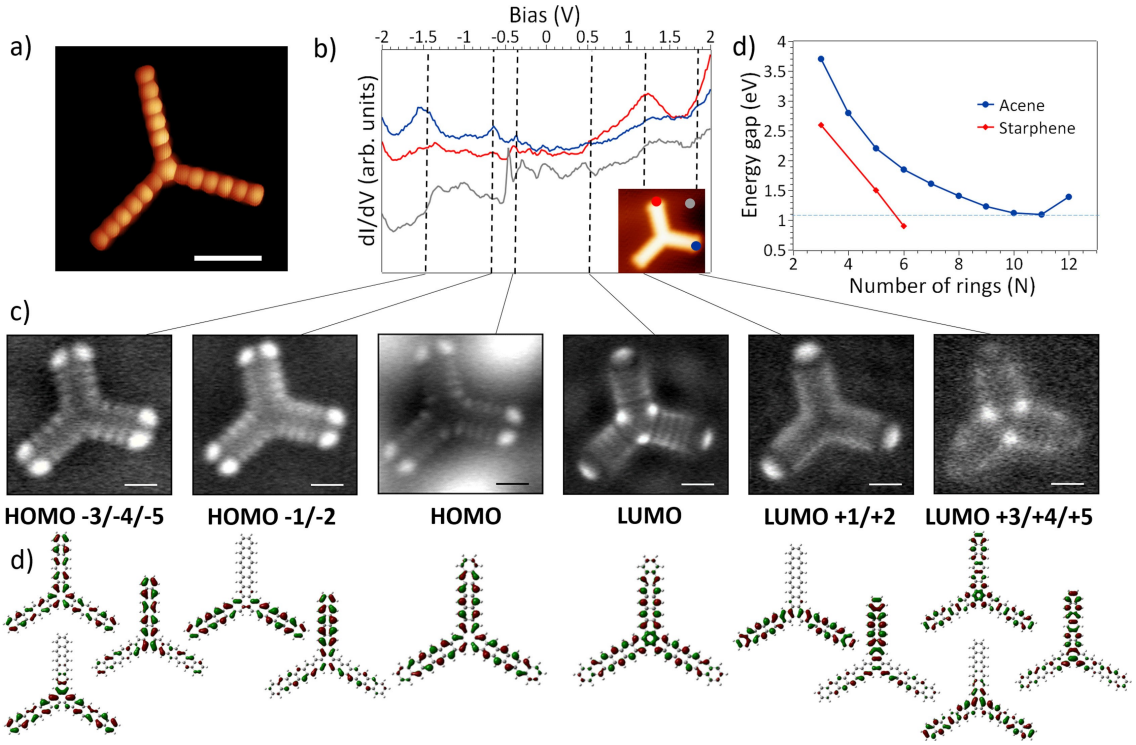

Figure 2. a) BR-STM image of [19]starphene **1** (scale bar: 1 nm). b) Differential conductance point spectra acquired on the molecule at the positions marked in the inset and on the bare surface. c) Conductance maps acquired at −1.42 eV, −0.64 eV, −0.36 eV, 0.54 eV, 1.2 eV and 1.85 eV (scale bars: 0.8 nm). d) Wavefunctions of the orbitals associated with each of the measured resonances and conduction maps in previous panels (DFT B3LYP/6-31g(d,p)). e) HOMO-LUMO gap as determined by scanning tunneling spectroscopy for starphenes and acenes of varying size. For a better comparison, the starphene size is given by the number of rings on each of its arms, the currently analyzed [19]starphene thus corresponding to N = 6. The dashed horizontal line marks the smallest acene gap reported to date, observed on undecacene.

Supporting Information for details). In analogy to Figure 2e, Figure 3a displays the calculated HOMO-LUMO gaps for acenes as a function of their number of rings N, and for starphenes as a function of the number of rings within each acene arm (thus corresponding to [3N + 1]starphenes). The calculations show qualitative resemblance to the experiments, with systematically lower HOMO-LUMO gap values for the (experimentally probed) starphenes and the value for N = 6 being smaller than that of any acene. However, for larger starphenes the gap increases and saturates towards the same value as the acene's gap (Figure 3a).

It is well-known that acenes develop an increasing radical character with an open-shell singlet ground state as they grow in size. Interestingly, the gradual change from closed-shell to open-shell character does not seem to cause major changes in the molecule's aromaticity, since NICS and HOMA values (Nucleus Independent Chemical Shift and Harmonic Oscillator of Model of Aromaticity, respectively) show only minimal changes with increasing size (Figure S22). One of the ways to quantify the radical character is by inspecting the occupation numbers of the (spinless) natural orbitals, which will always be 2 (doubly occupied) or 0 (unoccupied) for closed-shell molecules. As the occupancies depart from these numbers, an increasing open-shell character develops, reaching values close to 1 (single occupancy, unpaired electrons) in purely open-shell molecules. The calculated molecules start developing an open-shell character at a ring number marked in Figure 3a by the change from red to green symbols. This occurs at N = 7 for acenes and N = 6 for starphenes. It is important to note that different theoretical approaches may result in slightly different threshold N's.[16a,25] They all, however, display a smaller threshold for starphenes than for acenes.

Analyzing the natural orbital occupancies as a function of size, we also see other important differences between acenes and starphenes (Figures 3b-c). On the one hand, starphenes develop their open-shell character at a faster pace, with orbital occupancies close to 1 already for N = 8, whereas for acenes similar occupancies only occur for N = 10. On the other hand, at the onset of the developing open-shell character, acenes reveal partial occupations of the highest occupied natural orbital (HONO) and of the lowest unoccupied natural orbital (LUNO), and only at much larger sizes also of orbitals further from the Fermi level. Instead, for starphenes, the onset readily involves partial occupancies of the HONO and LUNO, as well as of the degenerate HONO-1/HONO-2 and the LUNO + 1/LUNO + 2. That is, whereas acenes initially develop a diradicaloid character for N = 7, starphenes develop a hexaradicaloid character starting with N = 6, which can be understood as two radicals emerging on each of the three acene arms. This analysis sets the basis for a simple picture of the studied molecules, that is based on a mean-field Hubbard model having only the above small set of relevant electronic states.

© 2024 The Author(s). Angewandte Chemie International Edition published by Wiley-VCH GmbH

15213773, 0, Downloaded from https://onlinelibrary.wiley.com/doi/10.1002/anie.202411861 by Uni Santiago Compostela, Wiley Online Library on [11/12/2024]. See the Terms and Conditions (https://onlinelibrary.wiley.com/terms-and-conditions) on Wiley Online Library for rules of use; OA articles are governed by the applicable Creative Commons License

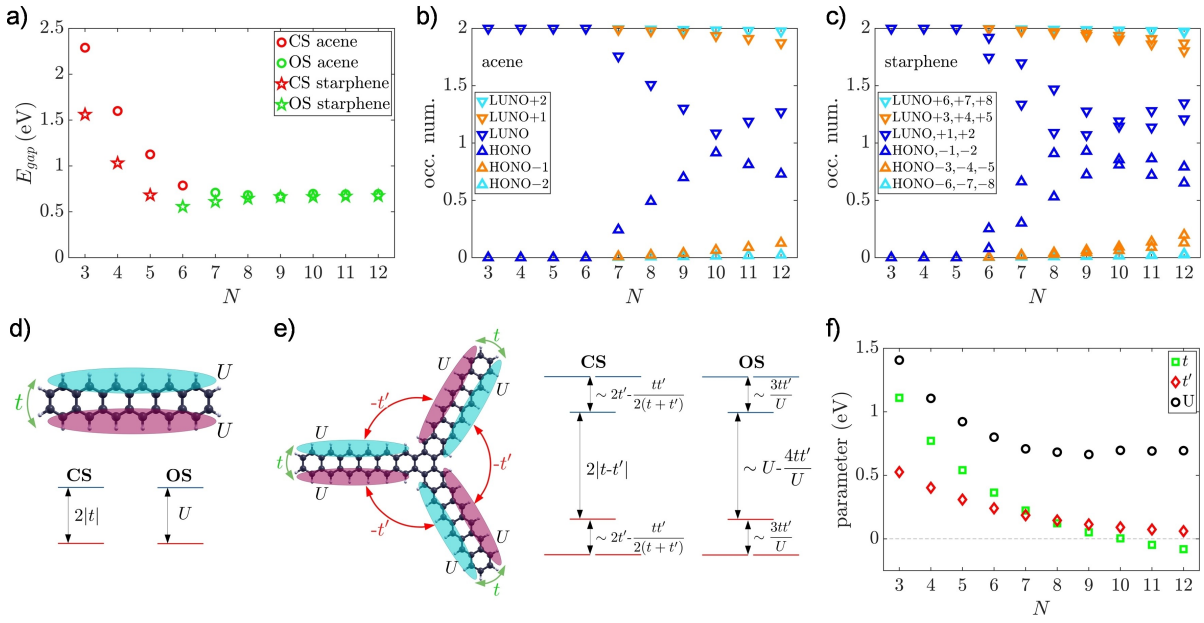

Figure 3. a) HOMO-LUMO gap for acenes (circles) and starphenes (stars) calculated as a function of size, where N denotes the number of rings in acenes and the number of rings per arm in starphenes. Whereas red symbols denote a purely closed-shell ground state, green symbols denote the development of a partial open-shell character. b) Occupancies of the low energy natural orbitals of acenes. c) Same as b), but for starphenes. d) Simplified model of acenes with two states interacting through a hopping integral *t* and an on-site interaction *U*, as well as the resulting HOMO-LUMO gaps for closed-shell (CS) and open-shell (OS) solutions. e) Simplified model of starphenes, with six states characterized by an "intra-arm" hopping integral *t*, an "inter-arm" hopping integral $-t$' an on-site interaction *U*, as well as the resulting HOMO-LUMO gaps for closed-shell (CS) and open-shell (OS) solutions. f) Size dependent values for *t*, *t*' and *U*, as obtained from fitting the DFT HOMO-LUMO and the simplified model gaps (see Supporting Information for details).

The acenes Hamiltonian includes two states interacting with a hopping integral t and an on-site Coulomb repulsion U (Figure 3d). Solving the Hamiltonian results in a HOMO-LUMO gap of $2|t|$ for a pure closed-shell system and of U for any partially open-shell one. The open-shell character arises then when $U>2|t|$. Fitting the DFT gaps with this model results in the size-dependent values for t and U depicted in Figure 3f (see Supporting Information for details).

The starphenes Hamiltonian includes two states per branch making a total of six states. Interactions between states in the same branch have the same hopping integral t and on-site interaction U as in the acenes Hamiltonian. Interactions between states in two different branches are characterized by a second "inter-arm" hopping integral t' (Figure 3e). The model delivers a HOMO-LUMO gap equal to $2|t-t'|$ for a closed-shell system and $\sim U - 4tt'/U$ for a pure open-shell system. Fitting the DFT gaps to the above expressions determines the size-dependent evolution of t' that is plotted in Figure 3f; this shows a smoothly decreasing trend that saturates towards 0 for large N. The decreasing behavior can be understood from the spreading of the density of states over the length of the arm. That is, the average distance between the electronic density of states on each arm increases with the molecular size, and the density of states in proximity to the central ring decreases as it spreads over longer arms.

The above t' behavior provides a qualitative explanation to our observations. For small N, the starphenes display a notably smaller HOMO-LUMO gap than the acenes that is caused by the "inter-arm" coupling. As the open-shell character develops for increasing N, the gap in starphene is still smaller than in acenes by $\sim 4tt'/U$, but the decreasing behavior of t' causes the gap to increase and saturate towards the same U value as in acenes. Since [19]starphene has the largest t' among all open-shell starphenes, it exhibits the smallest energy gap of the starphene family. As mentioned above for the development of an open-shell character, different theoretical approaches may also predict different starphene sizes for the lowest HOMO-LUMO gap. The experimental validation is on-going by the synthesis and characterization of a series of larger starphenes, which should at some point reveal both the HOMO-LUMO gap increase and the appearance of inelastic magnetic excitations in low energy conductance spectra. As a reference, on acenes the latter have only been observed for sizes $N \geq 13$.[16a]

Conclusion

All in all, we have shown two viable synthetic routes to obtain [19]starphene on a gold surface combining in-solution and on-surface synthesis. The subsequent characterization by scanning tunneling microscopy and spectroscopy has revealed a remarkably low HOMO-LUMO gap of only 0.9 eV. This is not only lower than the gap reported for hexacene, which forms each of its arms, but lower than that of any acene reported to date (comprising from naphthalene to tridecacene). Theoretical calculations explain these find-

© 2024 The Author(s). Angewandte Chemie International Edition published by Wiley-VCH GmbH

15213773, 0, Downloaded from https://onlinelibrary.wiley.com/doi/10.1002/anie.202411861 by Uni Santiago Compostela, Wiley Online Library on [11/12/2024]. See the Terms and Conditions (https://onlinelibrary.wiley.com/terms-and-conditions) on Wiley Online Library for rules of use; OA articles are governed by the applicable Creative Commons License

15213773, 0, Downloaded from https://onlinelibrary.wiley.com/doi/10.1002/anie.202411861 by Uni Santiago Compostela, Wiley Online Library on [11/12/2024]. See the Terms and Conditions (https://onlinelibrary.wiley.com/terms-and-conditions) on Wiley Online Library for rules of use; OA articles are governed by the applicable Creative Commons License

ings with an effective inter-arm coupling. Molecular size-dependent calculations reveal an increased radical character for starphenes as compared to acenes, whereas the HOMO-LUMO gap is predicted to saturate towards a common value. Importantly, the synthetic method to obtain [19]starphene can be directly extrapolated to larger sizes, setting the base to characterize and confirm their pronounced multiradical properties predicted by calculations.

Acknowledgements

The authors gratefully acknowledge financial support from Spanish MCIN/AEI/ 10.13039/501100011033 and the European Regional Development Fund (ERDF) through grants PID2022-140845OB-C6, PID2022-139933NB-I00 and PID2022-137078NB-100, from the European Union (EU) through Horizon 2020 (FET-Open project SPRING Grant. no. 863098), ERC SyG MolDAM (951519) and MSCA Postdoctoral Fellowship (Grant Agreement No. 101153230 to JPC), and from Xunta de Galicia (Centro de Investigación do Sistema Universitario de Galicia, 2023–2027, ED431G 2023/03).

Conflict of Interest

The authors declare no conflict of interest.

Data Availability Statement

The data that support the findings of this study are available from the corresponding author upon reasonable request.

[1] a) E. Clar, A. Mullen, *Tetrahedron* **1968**, *24*, 6719–6724; b) E. C. Rüdiger, M. Müller, J. Freudenberg, U. H. F. Bunz, *Org. Mater.* **2019**, *01*, 001–018.
[2] A. L. Kanibolotsky, I. F. Perepichka, P. J. Skabara, *Chem. Soc. Rev.* **2010**, *39*, 2695–2728.
[3] a) D. Skidin, O. Faizy, J. Krüger, F. Eisenhut, A. Jancarik, K.-H. Nguyen, G. Cuniberti, A. Gourdon, F. Moresco, C. Joachim, *ACS Nano* **2018**, *12*, 1139–1145; b) W. H. Soe, C. Manzano, P. de Mendoza, P. R. McGonigal, A. M. Echavarren, C. Joachim, *Surf. Sci.* **2018**, *678*, 163–168.
[4] a) C. Tönshoff, H. F. Bettinger, *Chem. Eur. J.* **2021**, *27*, 3193–3212; b) M. Müller, L. Ahrens, V. Brosius, J. Freudenberg, U. H. F. Bunz, *J. Mater. Chem. C* **2019**, *7*, 14011–14034.
[5] I. Pozo, E. Guitián, D. Pérez, D. Peña, *Acc. Chem. Res.* **2019**, *52*, 2472–2481.
[6] E. C. Rüdiger, S. Koser, F. Rominger, J. Freudenberg, U. H. F. Bunz, *Chem. Eur. J.* **2018**, *24*, 9919–9927.
[7] S. J. Hein, D. Lehnherr, W. R. Dichtel, *Chem. Sci.* **2017**, *8*, 5675–5681.
[8] P. T. Lynett, K. E. Maly, *Org. Lett.* **2009**, *11*, 3726–3729.
[9] E. C. Rüdiger, M. Porz, M. Schaffroth, F. Rominger, U. H. F. Bunz, *Chem. Eur. J.* **2014**, *20*, 12725–12728.
[10] a) S. Clair, D. G. de Oteyza, *Chem. Rev.* **2019**, *119*, 4717–4776; b) Q. Sun, R. Zhang, J. Qiu, R. Liu, W. Xu, *Adv. Mater.* **2018**, *30*, 1705630; c) A. Narita, Z. Chen, Q. Chen, K. Müllen, *Chem. Sci.* **2019**, *10*, 964–975.
[11] L. Gross, B. Schuler, N. Pavliček, S. Fatayer, Z. Majzik, N. Moll, D. Peña, G. Meyer, *Angew. Chem. Int. Ed.* **2018**, *57*, 3888–3908.
[12] a) P. Chen, D. Fan, A. Selloni, E. A. Carter, C. B. Arnold, Y. Zhang, A. S. Gross, J. R. Chelikowsky, N. Yao, *Nat. Commun.* **2023**, *14*, 1460; b) F. Albrecht, S. Fatayer, I. Pozo, I. Tavernelli, J. Repp, D. Peña, L. Gross, *Science* **2022**, *377*, 298–301; c) T. Wang, A. Berdonces-Layunta, N. Friedrich, M. Vilas-Varela, J. P. Calupitan, J. I. Pascual, D. Peña, D. Casanova, M. Corso, D. G. de Oteyza, *J. Am. Chem. Soc.* **2022**, *144*, 4522–4529.
[13] C. Sánchez-Sánchez, A. Nicolaï, F. Rossel, J. Cai, J. Liu, X. Feng, K. Müllen, P. Ruffieux, R. Fasel, V. Meunier, *J. Am. Chem. Soc.* **2017**, *139*, 17617–17623.
[14] J. Holec, B. Cogliati, J. Lawrence, A. Berdonces-Layunta, P. Herrero, Y. Nagata, M. Banasiewicz, B. Kozankiewicz, M. Corso, D. G. de Oteyza, A. Jancarik, A. Gourdon, *Angew. Chem. Int. Ed.* **2021**, *60*, 7752–7758.
[15] H. F. Bettinger, R. Mondal, D. C. Neckers, *Chem. Commun.* **2007**, 5209–5211.
[16] Very recently, two reports have described the generation of [13]acene, the largest acene obtained to date, on Au(111), showing gaps in the range of 1.1–1.4 eV. See: a) R. Zuzak, M. Kumar, O. Stoica, D. Soler-Polo, J. Brabec, K. Pernal, L. Veis, R. Blieck, A. M. Echavarren, P. Jelinek, S. Godlewski, *Angew. Chem. Int. Ed.* **2024**, *63*, e202317091; b) Z. Ruan, J. Schramm, J. B. Bauer, T. Naumann, H. F. Bettinger, R. Tonner-Zech, J. M. Gottfried, *J. Am. Chem. Soc.* **2024**, *146*, 3700–3709.
[17] a) J. Krüger, F. García, F. Eisenhut, D. Skidin, J. M. Alonso, E. Guitián, D. Pérez, G. Cuniberti, F. Moresco, D. Peña, *Angew. Chem. Int. Ed.* **2017**, *56*, 11945–11948; b) F. Eisenhut, T. Kühne, F. García, S. Fernández, E. Guitián, D. Pérez, G. Trinquier, G. Cuniberti, C. Joachim, D. Peña, F. Moresco, *ACS Nano* **2020**, *14*, 1011–1017.
[18] H. Haneda, S. Eda, M. Aratani, T. Hamura, *Org. Lett.* **2014**, *16*, 286–289.
[19] D. Peña, S. Escudero, D. Pérez, E. Guitián, L. Castedo, *Angew. Chem. Int. Ed.* **1998**, *37*, 2659–2661.
[20] J. Lawrence, A. Berdonces-Layunta, S. Edalatmanesh, J. Castro-Esteban, T. Wang, A. Jimenez-Martin, B. de la Torre, R. Castrillo-Bodero, P. Angulo-Portugal, M. S. G. Mohammed, A. Matěj, M. Vilas-Varela, F. Schiller, M. Corso, P. Jelinek, D. Peña, D. G. de Oteyza, *Nat. Chem.* **2022**, *14*, 1451–1458.
[21] T. Wang, S. Sanz, J. Castro-Esteban, J. Lawrence, A. Berdonces-Layunta, M. S. G. Mohammed, M. Vilas-Varela, M. Corso, D. Peña, T. Frederiksen, D. G. de Oteyza, *Nano Lett.* **2022**, *22*, 164–171.
[22] L. Colazzo, M. S. G. Mohammed, R. Dorel, P. Nita, C. García Fernández, P. Abufager, N. Lorente, A. M. Echavarren, D. G. de Oteyza, *Chem. Commun.* **2018**, *54*, 10260–10263.
[23] M. S. G. Mohammed, J. Lawrence, F. García, P. Brandimarte, A. Berdonces-Layunta, D. Pérez, D. Sánchez-Portal, D. Peña, D. G. de Oteyza, *Nanoscale Adv.* **2021**, *3*, 2351–2358.
[24] a) J. Krüger, F. Eisenhut, D. Skidin, T. Lehmann, D. A. Ryndyk, G. Cuniberti, F. García, J. M. Alonso, E. Guitián, D. Pérez, D. Peña, G. Trinquier, J.-P. Malrieu, F. Moresco, C. Joachim, *ACS Nano* **2018**, *12*, 8506–8511; b) W. H. Soe, C. Manzano, A. De Sarkar, N. Chandrasekhar, C. Joachim, *Phys. Rev. Lett.* **2009**, *102*, 176102; c) J. Krüger, F. Eisenhut, J. M. Alonso, T. Lehmann, E. Guitián, D. Pérez, D. Skidin, F. Gamaleja, D. A. Ryndyk, C. Joachim, D. Peña, F. Moresco, G. Cuniberti, *Chem. Commun.* **2017**, *53*, 1583–1586; d) R. Zuzak, R. Dorel, M. Kolmer, M. Szymonski, S. Godlewski, A. M. Echavarren, *Angew. Chem. Int. Ed.* **2018**, *57*, 10500–10505; e) J. I. Urgel, S. Mishra, H. Hayashi, J. Wilhelm, C. A. Pignedoli, M. Di Giovannantonio, R. Widmer, M. Yamashita, N. Hieda, P. Ruffieux, H. Yamada, R. Fasel, *Nat. Commun.* **2019**, *10*, 861; f) R. Zuzak, R. Dorel, M. Krawiec, B. Such, M.

 © 2024 The Author(s). Angewandte Chemie International Edition published by Wiley-VCH GmbH

Kolmer, M. Szymonski, A. M. Echavarren, S. Godlewski, *ACS Nano* **2017**, *11*, 9321–9329.
[25] a) M. Bendikov, H. M. Duong, K. Starkey, K. N. Houk, E. A. Carter, F. Wudl, *J. Am. Chem. Soc.* **2004**, *126*, 7416–7417; b) J. Hachmann, J. J. Dorando, M. Avilés, G. K.-L. Chan, *J. Chem. Phys.* **2007**, *127*; c) C.-N. Yeh, J.-D. Chai, *Sci. Rep.* **2016**, *6*, 30562; d) Y. Yang, E. R. Davidson, W. Yang, *Proc. Natl. Acad. Sci. USA* **2016**, *113*, E5098–E5107; e) T. Wang, P. Angulo-Portugal, A. Berdonces-Layunta, A. Jancarik, A. Gourdon, J. Holec, M. Kumar, D. Soler, P. Jelinek, D. Casanova, M. Corso, D. G. de Oteyza, J. P. Calupitan, *J. Am. Chem. Soc.* **2023**, *145*, 10333–10341.

Manuscript received: June 24, 2024
Accepted manuscript online: August 7, 2024
Version of record online: ■■, ■■

© 2024 The Author(s). Angewandte Chemie International Edition published by Wiley-VCH GmbH

15213773, 0, Downloaded from https://onlinelibrary.wiley.com/doi/10.1002/anie.202411861 by Uni Santiago Compostela, Wiley Online Library on [11/12/2024]. See the Terms and Conditions (https://onlinelibrary.wiley.com/terms-and-conditions) on Wiley Online Library for rules of use; OA articles are governed by the applicable Creative Commons License

Research Article

Starphene Chemistry

J. Besteiro-Sáez, L. M. Mateo, S. Salaverría, T. Wang, P. Angulo-Portugal, J. P. Calupitan, J. Rodríguez-Fernández, A. García-Fuente,* J. Ferrer, D. Pérez, M. Corso, D. G. de Oteyza,* D. Peña* _ **e202411861**

[19]Starphene: Combined In-Solution and On-Surface Synthesis Towards the Largest Starphene

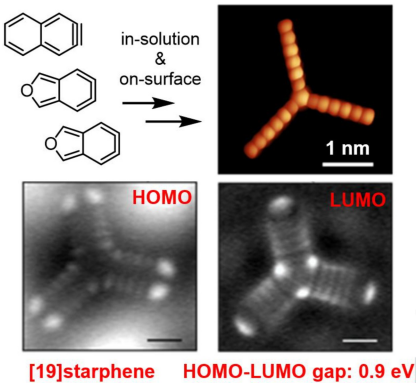

The synthesis of a star-shaped polyarene formed by 19 *cata*-fused benzene rings distributed within three hexacene branches is described. This molecule, which is the largest starphene that has been obtained to date, was prepared by combining in-solution and on-surface chemistry. [19]Starphene was characterized by high-resolution scanning tunneling microscopy (STM) and spectroscopy (STS) showing a remarkable small HOMO-LUMO transport gap (0.9 eV).

© 2024 The Author(s). Angewandte Chemie International Edition published by Wiley-VCH GmbH

15213773, 0, Downloaded from https://onlinelibrary.wiley.com/doi/10.1002/anie.202411861 by Uni Santiago Compostela, Wiley Online Library on [11/12/2024]. See the Terms and Conditions (https://onlinelibrary.wiley.com/terms-and-conditions) on Wiley Online Library for rules of use; OA articles are governed by the applicable Creative Commons License